《原子核物理评论》
www.npr.ac.cn Nuclear Physics Review
Started in 1984

等效质量模型中的重子质量谱

尤浩松 夏铖君 朱新梅 陈鹏辉 徐建峰 陆振烟 彭光雄 徐仁新

Baryon Spectra in the Framework of an Equivparticle Model

YOU Haosong, XIA Chengjun, ZHU Xinmei, CHEN Penghui, XU Jianfeng, LU Zhenyan, PENG Guangxiong, XU Renxin

在线阅读 View online: https://doi.org/10.11804/NuclPhysRev.39.2022111

引用格式:
尤浩松, 夏铖君, 朱新梅, 陈鹏辉, 徐建峰, 陆振烟, 彭光雄, 徐仁新. 等效质量模型中的重子质量谱[J]. 原子核物理评论, 2022, 39(3):302-310. doi: 10.11804/NuclPhysRev.39.2022111
YOU Haosong, XIA Chengjun, ZHU Xinmei, CHEN Penghui, XU Jianfeng, LU Zhenyan, PENG Guangxiong, XU Renxin. Baryon Spectra in the Framework of an Equivparticle Model[J]. Nuclear Physics Review, 2022, 39(3):302-310. doi: 10.11804/NuclPhysRev.39.2022111

Article ID: 1007-4627(2022)03–0302–09

Baryon Spectra in the Framework of an Equivparticle Model

YOU Haosong[1], XIA Chengjun[1,†], ZHU Xinmei[1], CHEN Penghui[1], XU Jianfeng[2], LU Zhenyan[3], PENG Guangxiong[4,5,6], XU Renxin[7,8]

(*1. College of Physical Science and Technology, Yangzhou University, Yangzhou 225009, Jiangsu, China*;
2. College of information Engineering, Suqian University, Suqian 223800, Jiangsu, China;
3. School of Physics and Electronics, Hunan University of Science and Technology, Xiangtan 411201, Hunan, China;
4. School of Nuclear Science and Technology, University of Chinese Academy of Sciences, Beijing 100049, China;
5. Theoretical Physics Center for Science Facilities, Institute of High Energy Physics, Beijing 100049, China;
6. Synergetic Innovation Center for Quantum Effects and Application, Hunan Normal University, Changsha 410081, China;
7. School of Physics, Peking University, Beijing 100871, China;
8. Kavli Institute for Astronomy and Astrophysics, Peking University, Beijing 100871, China)

Abstract: Based on an equivparticle model incorporating both confinement and leading-order perturbative interactions, we fit the model parameters to the experimental masses of p, n, Λ, and Δ. It is found that the equivparticle model well reproduces the mass spectra of light baryons. Distinctive correlations of the confinement strength D, the strong coupling constant α_s, and quark mass factor f with respect to the perturbative strength C are obtained, which can be well approximated by analytical formulae. The color-magnetic part of one-gluon-exchange interaction plays a significant role on the mass spectra of light baryons, which causes a mass gap of up to 300 MeV between baryons with spins $J = 1/2$ and 3/2. By adopting different strong coupling constants for a pair of quarks with strangeness, the hyperon masses can be better described with the model parameters fitted to the masses of Σ and Ξ. The equivparticle model developed here with constrained parameter sets are then applicable to the investigation of exotic states such as udQM nuggets, strangelets, and compact stars.

Key words: baryon spectra; equivparticle model; one-gluon-exchange interaction

CLC number: O571 **Document code:** A **DOI:** 10.11804/NuclPhysRev.39.2022111

1 Introduction

Quantum Chromodynamics(QCD) predicts the existence of quark states beyond mesons and baryons, where the number of quarks can exceed three, *e.g.*, multiquark states, multibaryons, nuggets and compact stars made of quark matter. However, due to its nonperturbative nature and infamous sign problem in lattice simulations, currently we have to rely on various QCD inspired effective models to unveil the properties of those objects. For example, the multibaryons were investigated with the bag model[1–7], nonrelativistic quark cluster model[8–11], Skyrme model[12–15], and diquark model[16]. The interaction among multibaryons with strangeness, *i.e.*, strangeons, were investigated with quark cluster model[17], extended σ-ω-ρ mean-field model[18], Lennard-Jones potential model[19], linked bag model[20–21], and so on. The properties of quark matter were examined in the framework of bag model[22–23], Nambu-Jona-Lasinio (NJL) model[24], perturbation model[25], field correlator method[26], quasiparticle model[27–32], equivparticle model[33–37], *etc*.

These models, to some extent, have large ambiguities on their predictions of exotic quark states as the model parameters and assumptions are not very well constrained. For example, the H-dibaryons were speculated to be a stable state in the bag model[1–2], while recent lattice QCD simulations suggests H-dibaryons are weakly bound or unbound[38–39]. In a large parameter space in models such as bag model, it was shown that strange quark matter (SQM) comprised of approximately equal numbers of u, d, and s quarks are more stable than nuclear matter[40–43], which permits the existence of strangelets[23, 44–46], nuclear-

Received date: 02 Aug. 2022; **Revised date:** 20 Aug. 2022

Foundation item: National SKA Program of China(2020SKA0120300, 2020SKA0120100); National Natural Science Foundation of China(12275234, 12105241, 11875052, 12005005, 12205093, 11673002); Scientific Research Start-up Fund of Talent Introduction of Suqian University No. Xiao2022XRC061

Biography: YOU Haosong(2003–), Male, Wuxi, Jiangshu Province, undergraduate student, working on high energy nuclear physics

† **Corresponding author:** XIA Chengjun, E-mail: cjxia@yzu.edu.cn

ites[47−48], meteorlike compact ultradense objects[49], and strange stars[50−52]. However, in models with spontaneous chiral symmetry breaking, SQM is unstable[53−54], while the nonstrange quark matter (udQM) could be the true ground state[55]. In such cases, there may be udQM nuggets[55−57] and nonstrange quark stars[58−63].

Due to the large uncertainties in model predictions and their significant implications, it is essential to constrain the model parameters according to various experimental and observational data. The purpose of our current study is thus to constrain the model parameters of equivparticle model according to the experimental mass spectra of light baryons with spins $J = 1/2$ and 3/2. For those consistent with the experimental baryon masses, distinctive correlations between the model parameters are identified. The color-magnetic part of one-gluon-exchange interaction was shown to play an important role on the mass spectra of light baryons, which becomes weaker for baryons with strangeness. The model parameters fixed here can be readily applied to the investigation of exotic states such as udQM nuggets, strangelets, and compact stars.

The paper is organized as follows. In Sec. 2 we present the theoretical framework of the equivparticle model, where the properties of baryons are obtained in mean field approximations with quarks occupying the $1s_{1/2}$ orbits. The numerical results that best reproduce the baryon spectra are then presented in Sec. 3, where the correlations of the confinement strength D, the strong coupling constant α_s, and quark mass factor f with respect to the perturbative strength C are identified and indicated with analytical formulae. We draw our conclusion in Sec. 4.

2 Theoretical framework

2.1 Quark mass scaling

In the framework of equivparticle model[33−37, 64−79], the strong interactions among quarks are accounted for with density and/or temperature dependent quark masses, where the mass of quark i is fixed with

$$m_i = m_{i0} + m_{\rm I}(\{n_j\}, T). \tag{1}$$

Here n_j represents the number density for quark flavor j, T the temperature, and $m_{\rm u0} = 2.16$ MeV, $m_{\rm d0} = 4.67$ MeV, $m_{\rm s0} = 93$ MeV the current masses of quarks[80−81]. To reflect the effects of quark confinement as in bag model, the density dependent quark masses for zero temperature cases are parametrized as[33, 35]

$$m_{\rm I}(n_{\rm b}) = \frac{B}{3n_{\rm b}}, \tag{2}$$

where B is the bag constant and $n_{\rm b} = \sum_{i={\rm u,d,s}} n_i/3$ the baryon number density. Alternatively, a cubic-root scaling is derive from the linear confinement and leading-order in-medium chiral condensate[64], *i.e.*,

$$m_{\rm I}(n_{\rm b}) = Dn_{\rm b}^{-1/3}, \tag{3}$$

where $D = -3(2/\pi)^{1/3}\sigma n^*/\sum_{\rm q}\langle\bar{\rm q}{\rm q}\rangle_0$ represents the confinement strength with σ being the string tension, $n^* \approx 0.49$ fm^{-3} the chiral restoration density in the linear expression[82], and $\sum_{\rm q}\langle\bar{\rm q}{\rm q}\rangle_0$ the sum of vacuum chiral condensates. Further consideration of one-gluon-exchange interaction suggests[71]

$$m_{\rm I}(n_{\rm b}) = Dn_{\rm b}^{-1/3} - Cn_{\rm b}^{1/3}, \tag{4}$$

while $C = -4(2/\pi)^{1/3}\alpha_{\rm s}n^*/\sum_{\rm q}\langle\bar{\rm q}{\rm q}\rangle_0$ varies with the strong coupling constant $\alpha_{\rm s}$. Incorporating the leading-order perturbative interactions at ultrahigh densities, we have found[75]

$$m_{\rm I}(n_{\rm b}) = Dn_{\rm b}^{-1/3} + Cn_{\rm b}^{1/3}, \tag{5}$$

where the perturbative strength $C \approx \pi^{2/3}\sqrt{\frac{2\alpha_{\rm s}}{3\pi}}$. An isospin dependent term was also introduced to examine the impacts of quark matter symmetry energy, which was given by

$$m_i(n_{\rm b}, \delta) = m_{i0} + Dn_{\rm b}^{-1/3} - \tau_i\delta D_I n_{\rm b}^{\alpha}{\rm e}^{-\beta n_{\rm b}} \tag{6}$$

with τ_i being the third component of isospin for quark flavor i and $\delta = 3(n_{\rm d} - n_{\rm u})/(n_{\rm d} + n_{\rm u})$ the isospin asymmetry[76]. Recently, we have proposed a similar mass scaling[57]

$$m_{\rm I}(n_{\rm b}, \delta) = Dn_{\rm b}^{-1/3} + Cn_{\rm b}^{1/3} + C_I\delta^2 n_{\rm b}, \tag{7}$$

where C_I corresponds to the strength of symmetry energy and is sensitive to the strong interactions among quarks[62−63, 76, 83−86].

2.2 Lagrangian density

The Lagrangian density of the equivparticle model is determined by

$$\mathcal{L} = \sum_i \bar{\psi}_i\left[{\rm i}\gamma^\mu\partial_\mu - m_i - eq_i\gamma^\mu A_\mu\right]\psi_i - \frac{1}{4}A_{\mu\nu}A^{\mu\nu}, \tag{8}$$

where ψ_i represents the Dirac spinor of quark flavor i, m_i the mass, q_i the charge ($q_{\rm u} = 2e/3$ and $q_{\rm d} = q_{\rm s} = -e/3$), and A_μ the photon field with the field tensor

$$A_{\mu\nu} = \partial_\mu A_\nu - \partial_\nu A_\mu. \tag{9}$$

The strong interactions are considered with density-dependent quark masses in equivparticle model, where the quark mass in Eq. (8) varies with baryon number density, *i.e.*,

$$m_i(n_{\rm b}) = fm_{i0} + Dn_{\rm b}^{-1/3} + Cn_{\rm b}^{1/3}. \tag{10}$$

Note that we have considered both the linear confinement and leading-order perturbative interactions as in Eq. (5),

while the current quark masses m_{i0} are multiplied by a factor f to account for the running quark masses.

Adopting the Euler-Lagrange equation, one obtains the equation of motion for quarks

$$\gamma^{\mu}\left(\mathrm{i}\partial_{\mu}-\mathrm{eq_i A}_{\mu}-\mathrm{V_V}\delta_{\mu 0}\right)\psi_i = m_i\psi_i. \tag{11}$$

The term V_V arises from the density dependent quark masses, *i.e.*,

$$V_V = \frac{1}{3}\frac{\mathrm{d}m_{\mathrm{I}}}{\mathrm{d}n_{\mathrm{b}}}\sum_i \bar{\psi}_i\psi_i. \tag{12}$$

The equation of motion for photons is given by

$$\Box A^{\mu} = e\sum_i q_i\bar{\psi}_i\gamma^{\mu}\psi_i = e\sum_i J_i^{\mu e}. \tag{13}$$

2.3 Spherical case

For a spherically symmetric system, the Dirac spinor of quarks can be expanded as

$$\psi_{n\kappa m}(\boldsymbol{r}) = \frac{1}{r}\begin{pmatrix} \mathrm{iG_{n\kappa}(r)} \\ F_{n\kappa}(r)\boldsymbol{\sigma}\cdot\hat{\boldsymbol{r}} \end{pmatrix} Y^l_{jm}(\theta,\phi), \tag{14}$$

with $G_{n\kappa}(r)/r$ and $F_{n\kappa}(r)/r$ being the radial wave functions for the upper and lower components, while $Y^l_{jm}(\theta,\phi)$ is the spinor spherical harmonics, *i.e.*,

$$Y^l_{jm} = \sum_{l_z,s_z}\langle l, l_z; 1/2, s_z|j, m\rangle Y_{ll_z}\chi^{s_z}_{1/2}. \tag{15}$$

The quantum number κ is defined by the angular momenta (l, j) as $\kappa = (-1)^{j+l+1/2}(j+1/2)$. The Dirac equation for the radial wave functions in mean-field approximation is then fixed by

$$\begin{pmatrix} V_i+m_i & -\dfrac{\mathrm{d}}{\mathrm{d}r}+\dfrac{\kappa}{r} \\ \dfrac{\mathrm{d}}{\mathrm{d}r}+\dfrac{\kappa}{r} & V_i-m_i \end{pmatrix}\begin{pmatrix} G_{n\kappa} \\ F_{n\kappa} \end{pmatrix} = \varepsilon_{n\kappa}\begin{pmatrix} G_{n\kappa} \\ F_{n\kappa} \end{pmatrix} \tag{16}$$

with the single particle energy $\varepsilon_{n\kappa}$ and the mean-field vector potential

$$V_i = V_V + eq_iA_0 = \frac{1}{3}\frac{\mathrm{d}m_{\mathrm{I}}}{\mathrm{d}n_{\mathrm{b}}}\sum_{i=\mathrm{u,d,s}} n_i^{\mathrm{s}} + eq_iA_0. \tag{17}$$

For given radial wave functions, the scalar and vector densities of quarks can be determined by

$$n_i^{\mathrm{s}}(r) = \frac{1}{4\pi r^2}\sum_{k=1}^{N_i}\left[|G_{ki}(r)|^2 - |F_{ki}(r)|^2\right], \tag{18a}$$

$$n_i(r) = \frac{1}{4\pi r^2}\sum_{k=1}^{N_i}\left[|G_{ki}(r)|^2 + |F_{ki}(r)|^2\right], \tag{18b}$$

where the quark numbers N_i $(i = \mathrm{u, d, s})$ are obtained by integrating the density $n_i(r)$ in coordinate space as

$$N_i = \int 4\pi r^2 n_i(r)\mathrm{d}r. \tag{19}$$

The energy of the system can be obtained with

$$E_0 = \sum_{i,k=1}^{N_i}\varepsilon_{ki} - \int 2\pi r^2[6n_{\mathrm{b}}V_V + en_{\mathrm{ch}}A_0]\mathrm{d}r. \tag{20}$$

For given C, D and f, we solve the Dirac Eq. (16), mean field potential Eq. (17), and densities Eq. (18) inside a box by iteration in coordinate space with the grid width 0.001 fm. The box size varies with quark numbers and is fixed at vanishing densities.

2.4 Center-of-mass correction

The obtained solution for a baryon can be viewed as a wave packet of the physical particle with various total momentum $\boldsymbol{P}$, where the actual mass M_0 can be approximately obtained with[87]

$$E_0 = \left\langle\sqrt{M_0^2+P^2}\right\rangle \approx \sqrt{M_0^2+\langle P^2\rangle}. \tag{21}$$

The energy E_0 is determined by Eq. (20). And the expectation value of the squared total momentum $\langle P^2\rangle$ is obtained as in Ref. [88]. Then the center-of-mass corrections are introduced via the parameter Γ with

$$\frac{1}{\Gamma} = \left\langle\frac{1}{\gamma}\right\rangle = \left\langle\sqrt{1-v^2}\right\rangle \approx \sqrt{1-\frac{\langle P^2\rangle}{E_0^2}}. \tag{22}$$

Finally, the mean-square radius and mass are obtained with

$$\langle r^2\rangle = \left[\langle r^2\rangle_0 - \frac{9Q}{4M_0^2(\Gamma^2-1)}\right]\frac{3\Gamma^2}{2\Gamma^2+1}, \tag{23}$$

$$M_0 = \frac{E_0}{\Gamma}, \tag{24}$$

where M_0 stands for the mass of the corresponding baryon and Q the charge number.

2.5 One-gluon-exchange interactions

The one-gluon-exchange interaction is treated as a correction to the mass of Eq. (24), which is obtained with

$$\Delta M = \sum_{i<j}\alpha_{\mathrm{s}}^{ij}\iint\frac{\mathrm{d}^3r_i\mathrm{d}^3r_j}{|\boldsymbol{r_i}-\boldsymbol{r_j}|}\langle J_i^{\mu C}(\boldsymbol{r_i})J^C_{\mu,j}(\boldsymbol{r}_j)\rangle. \tag{25}$$

According to the quark wave functions in Eq. (14), the color current of quark i is given by

$$J_i^{0C}(\boldsymbol{r_i}) = \frac{\lambda_i^C}{2}\frac{1}{r_i^2}I_i(r_i)|Y^l_{jm}(\theta,\phi)|^2, \tag{26}$$

$$\boldsymbol{J}_i^C(\boldsymbol{r_i}) = \frac{\lambda_i^C}{2}\frac{1}{r_i^2}M_i(r_i)|Y^l_{jm}(\theta,\phi)|^2\left(\frac{\boldsymbol{r}_i}{r_i}\times\boldsymbol{\sigma_i}\right), \tag{27}$$

where

$$I_i(r_i) = |G_i(r_i)|^2 + |F_i(r_i)|^2, \tag{28}$$

$$M_i(r_i) = G_i^*(r_i)F_i(r_i) + G_i(r_i)F_i^*(r_i). \tag{29}$$

The one-gluon-exchange interaction can be divided into the color-electric and -magnetic parts. To simplify our calculation, we neglect the self-energy diagram and the color-electric part of one-gluon-exchange interaction, which are expected to be included in the quark mass scaling[71]. For the cases with $l=0$ (occupying the $1s_{1/2}$ state), we have $|Y^l_{jm}(\theta,\phi)|^2 = 1/4\pi$. Then Eq. (25) for baryons is finally reduced to

$$\Delta M = \sum_{i<j} \frac{2\alpha_s^{ij}}{3} a_{i,j} \int_0^R M_i(r_i) \int_0^{r_i} \frac{M_j(r)}{r} \mathrm{d}r\mathrm{d}r_i. \tag{30}$$

The interaction coefficients from quark spins are fixed with

$$a_{i,j} = \left\langle \boldsymbol{\sigma}_i \cdot \boldsymbol{\sigma}_j \right\rangle = 2S_{i,j}(S_{i,j}+1) - 3, \tag{31}$$

where $S_{i,j} = 0$ or 1 is the total spin of the pair of quarks i and j. The total baryon mass is finally obtained by adding the corrections to Eq. (24), *i.e.*,

$$M = M_0 + \Delta M. \tag{32}$$

3 Results and discussions

Based on the formulae introduced in Sec. 2, the baryon masses are then fixed by Eq. (32), which include both the center-of-mass corrections in Eq. (24) and color-magnetic part of one-gluon-exchange interactions in Eq. (30). We then fit to the mass spectra of baryons with angular momentum $l=0$ and masses $M<1.35$ GeV at $C=-1$, -0.5, -0.2, 0, 0.2, 0.5, 0.7, 1, where the experimental baryon masses are taken from Particle Data Group[81]. The obtained parameter sets that best reproduce the experimental values are indicated in Table 1.

Table 1　The parameter sets that best fit the experimental baryon spectra for the quark mass scaling in Eq. (10) and the strong coupling constants. The current masses of quarks are taken as $m_{u0} = 2.16^{+0.49}_{-0.26}$ MeV, $m_{d0} = 4.67^{+0.48}_{-0.17}$ MeV, and $m_{s0} = 93^{+11}_{-5}$ MeV[80-81].

C	$\sqrt{D}$	f	α_s^{ll}	α_s^{ls}	α_s^{ss}
−1	190.06	2.79	0.654	0.476	0.170
−0.5	169.44	2.50	0.857	0.621	0.299
−0.2	157.30	2.50	1.026	0.774	0.149
0.0	150.59	2.39	1.155	0.857	0.237
0.2	144.58	2.32	1.321	0.995	0.296
0.5	135.42	2.28	1.610	1.230	0.197
0.7	130.12	2.24	1.846	1.421	0.194
1.0	122.88	2.19	2.287	1.778	0.178

To illustrate our results, in Fig. 1 we present the obtained baryon masses by taking $C=-1$, 0, 0.7, and 1, where the corresponding parameter sets are listed in Table 1. In particular, we first fix the parameters D, f, and α_s^{ll} ($l=$ u,d) by reproducing the masses of p, n, Λ, and Δ. According to the quark mass scaling in Eq. (10), the confinement (D) and perturbative (C) interactions provide the bulk properties of baryon mass spectra, where a distinctive C-D correlation can be obtained. The fine structures such as the mass differences between nucleons N (p, n) and Λ-hyperons $\Delta M_{N\Lambda}$ determines f, while $\Delta M_{N\Delta}$ determines the strong coupling constant α_s^{ll} for the color-magnetic part of one-gluon-exchange interaction. Based on those parameter sets and assuming unified strong coupling constants $\alpha_s^{ss} = \alpha_s^{ls} = \alpha_s^{ll}$, we then estimate the masses of other baryons, which are indicated by the dots connected by dashed lines in Fig. 1. It is evident that our model slightly underestimates the masses of Σ, Ξ and overestimates the masses of their excited states Σ*, Ξ* as well as Ω. The slight deviations from the experimental baryon masses could be attributed to the variation of strong coupling constant on quark masses, which is in principle running with the energy scale.

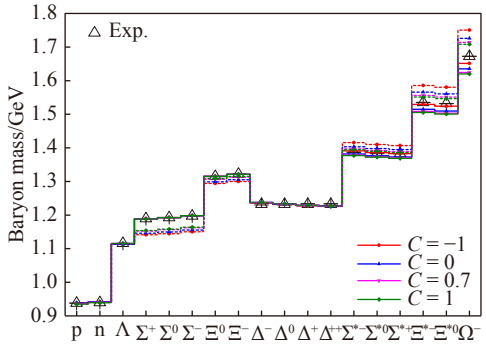

Fig. 1　The obtained masses of baryons consisting of light quarks adopting the parameter sets indicated in Table 1. The dots connected by dashed lines are fixed by taking unified values for strong coupling constants $\alpha_s^{ss} = \alpha_s^{ls} = \alpha_s^{ll}$, while those connected by the solid lines (indicated in Table 2) adopt strong coupling constants that vary with the contents of interacting quark pairs.(color online)

To better reproduce the mass spectra of light baryons, we thus adopt different strong coupling constants for quark pairs with strangeness, *i.e.*, $\alpha_s^{ss} \neq \alpha_s^{ls} \neq \alpha_s^{ll}$. The strong coupling constants are then fixed by fitting α_s^{ls} to the mass of Σ^0 and α_s^{ss} to the masses of Ξ, which are indicated in Table 1. Then the mass corrections ΔM from the color-magnetic part of one-gluon-exchange interactions are modified for Σ, Ξ, Σ*, Ξ* and Ω. The obtained mass spectra are indicated by the dots connected by the solid curves in Fig. 1, where the agreement between predicted and experimental values is obviously improved. In particular, the experimental values of baryons with $M<1.5$ GeV are well reproduced. For more massive baryons Ξ* and Ω, our model slightly under-

estimates their masses. Nevertheless, the deviation decreases if we adopt negative C, which in principle incorporates the color-electric part of one-gluon-exchange interactions[71].

The numerical results correspond to the dots connected by the solid curves in Fig. 1 are presented in Table 2. The root-mean-square deviations σ from the experimental values of $N = 18$ baryons are indicated, which are fixed by

$$\sigma = \sqrt{\sum_{i=1}^{N}(M^i_{\rm cal} - M^i_{\rm exp})^2/N} \tag{33}$$

with $M^i_{\rm cal}$ and $M^i_{\rm exp}$ being the numerical and experimental baryon masses. It is found that σ is generally on the order of 10 MeV and increase with C. Note that for baryons with spin $J = 1/2$, quarks form pairs with total spin $S = 0$ and 1 as indicated in Table 2, which determines the interaction coefficients $a_{i,j}$ for the color-magnetic part of one-gluon-exchange interaction in Eq. (31). For baryons with spin $J = 3/2$, all three quarks' spins are aligned.

In Fig. 2 we present the center-of-mass correction parameter Γ, the root-mean-square radius $\sqrt{\langle r^2\rangle}$ and the mass correction ΔM from the color-magnetic part of one-

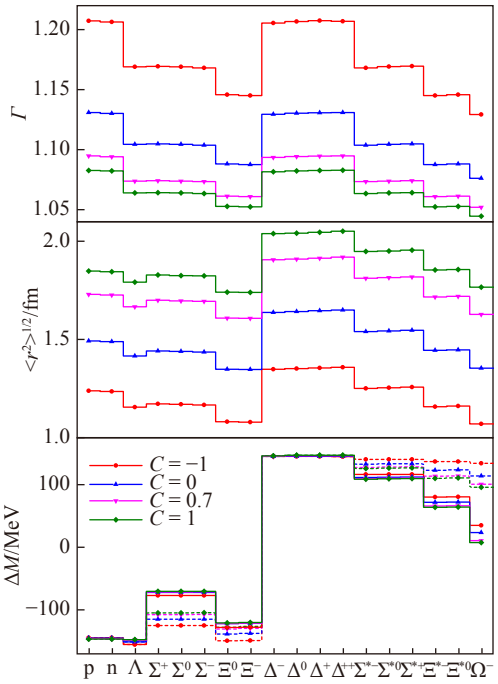

Fig. 2 The center-of-mass correction parameter Γ, the root-mean-square radius $\sqrt{\langle r^2\rangle}$ and the mass correction ΔM from the color-magnetic part of one-gluon-exchange interactions obtained with Eqs. (22), (23) and (30). (color online)

Table 2 The masses $M_{\rm cal}$ for baryons with given spins J and parities P, which are obtained with Eq. (32) adopting the parameter sets listed in Table 1. For baryons with $J^P = \frac{1}{2}^+$, the quark pair q_j and q_k with a total spin S is indicated by $\mathrm{q}_i(\mathrm{q}_j\mathrm{q}_k)_S$, which determines the interaction coefficients according to Eq. (31). The root-mean-square deviation σ (in MeV) for each parameter sets are presented, where the experimental masses $M_{\rm exp}$ are taken from the Particle Data Group[81].

J^P	Baryon	Quark content	$M_{\rm exp}$/MeV	$M_{\rm cal}$/MeV			
				$C=-1$	$C=0$	$C=0.7$	$C=1$
$\frac{1}{2}^+$	p	$\mathrm{u(ud)_0}$	938.272 046(21)	938.0	938.0	936.4	935.5
	n	$\mathrm{d(ud)_0}$	939.565 379(21)	941.4	941.8	940.5	939.7
	Λ	$\mathrm{s(ud)_0}$	1 115.683(6)	1 114.5	1 113.7	1 115.6	1 115.5
	Σ^+	$\mathrm{s(uu)_1}$	1 189.37(7)	1 189.4	1 188.9	1 188.6	1 188.5
	Σ^0	$\mathrm{s(ud)_1}$	1 192.642(24)	1 192.6	1 192.6	1 192.6	1 192.6
	Σ^-	$\mathrm{s(dd)_1}$	1 197.449(30)	1 198.1	1 198.1	1 198.1	1 198.1
	Ξ^0	$\mathrm{u(ss)_1}$	1 314.86(20)	1 315.4	1 315.3	1 315.2	1 315.2
	Ξ^-	$\mathrm{d(ss)_1}$	1 321.71(7)	1 321.2	1 321.3	1 321.4	1 321.4
$\frac{3}{2}^+$	Δ^-	ddd	1 232(2)	1 236.9	1 237.3	1 237.2	1 237.5
	Δ^0	udd	1 232(2)	1 231.4	1 232.3	1 232.6	1 233.0
	Δ^+	uud	1 232(2)	1 227.8	1 228.5	1 228.8	1 229.2
	Δ^{++}	uuu	1 232(2)	1 226.2	1 226.3	1 226.0	1 226.3
	Σ^{*-}	dds	1 387.2(5)	1 391.4	1 381.8	1 378.8	1 377.0
	Σ^{*0}	uds	1 383.7(10)	1 386.1	1 376.8	1 374.0	1 372.4
	Σ^{*+}	uus	1 382.80(35)	1 382.7	1 373.2	1 370.3	1 368.6
	Ξ^{*-}	dss	1 535.0(6)	1 529.3	1 514.6	1 508.3	1 505.2
	Ξ^{*0}	uss	1 531.80(32)	1 524.1	1 509.6	1 503.4	1 500.4
	Ω^-	sss	1 672.45(29)	1 651.3	1 635.3	1 624.2	1 620.2
		$\sigma = \sqrt{\sum_i (M^i_{\rm cal} - M^i_{\rm exp})^2/N}$		6.0	11.9	15.4	16.8

gluon-exchange interaction, which are in correspondence to the baryon spectra indicated in Fig. 1 and Table 2. For baryons obtained with different parameter sets, it is found that the center-of-mass correction parameter Γ is generally inversely proportional to the root-mean-square radius $\sqrt{\langle r^2\rangle}$, which is due to the enhancement of kinetic energy of quarks as baryons become more compact. Nevertheless, the variation of Γ share similar trends as that of $\sqrt{\langle r^2\rangle}$, where the strange quark mass plays the leading role. The mass corrections ΔM of p, n, Λ, and Δ from the color-magnetic part of one-gluon-exchange interactions are invariant to the adopted parameter set, which is mainly because we fit our parameter sets based on those baryons. If we examine other baryons, as indicated by the dashed lines, slight variations are observed for hyperons when we take $\alpha_s^{ss}=\alpha_s^{ls}=\alpha_s^{ll}$ (dashed lines). Similar situation is observed if we take $\alpha_s^{ss}\neq\alpha_s^{ls}\neq\alpha_s^{ll}$, where ΔM varies little for Σ and Ξ since α_s^{ls} and α_s^{ss} are fixed according to their masses. This suggests that the mass correction ΔM from the color-magnetic part of one-gluon-exchange interactions is insensitive to the adopted model parameters, which are expected to play important roles in color superconductivity in dense quark matter[89], the strength of symmetry energy coefficient C_I of quark matter as in Eq. (7), as well as the strong interactions among baryons[90].

As indicated in Table 1, we have considered additional four parameter sets with $C=-0.5$, -0.2, 0.2, and 0.5, where the parameters D, f, α_s^{ll}, α_s^{ls}, and α_s^{ss} are fixed in a same manner. The parameters that best reproduce the experimental baryon spectra are then plotted in Fig. 3, which can be well approximated by the following formulae, *i.e.*,

$$\sqrt{D}=90\times1.443^{-C}+60.5, \tag{34}$$

$$\alpha_s^{ll}=0.97\times2.14^{C}+0.2, \tag{35}$$

$$f=1.27^{-C}+1.4, \tag{36}$$

$$\alpha_s^{ls}=0.79\times2.14^{C}+0.09, \tag{37}$$

$$\alpha_s^{ss}=0.2. \tag{38}$$

It is found that the confinement strength D (in MeV^2) decreases with the perturbative strength C, which is attributed to the fixed masses of baryons as both confinement and perturbative interactions contribute positively to the total mass. The mass factor f ranges from 2.19 to 2.79, suggesting the strange quark mass should be at least 210 MeV to account for the mass difference between N and Λ. This has significant implications on the stability of strange quark matter, where ud quark matter might be more stable[55]. Meanwhile, we note f decreases slightly with C, where the mass difference $\Delta M_{N\Lambda}$ is mainly from fm_{s0} instead of its kinetic energy as the baryons become less compact. In this work, we have considered two scenarios for the strong coupling constants of one-gluon-exchange interactions, *i.e.*, a unified value with $\alpha_s=\alpha_s^{ss}=\alpha_s^{ls}=\alpha_s^{ll}$ and flavor-dependent ones with $\alpha_s^{ss}\neq\alpha_s^{ls}\neq\alpha_s^{ll}$. To better describe the masses of hyperons, it is found that $\alpha_s^{ss}<\alpha_s^{ls}<\alpha_s^{ll}$, which is reasonable as α_s should decrease with the total mass of each quark pair. Meanwhile, the strong coupling constants generally increase with C, which may be attributed to the running coupling constant with respect to the density or radius, *e.g.,* those in Ref. [91].

The relative differences between our calculation and the experimental baryon masses are indicated in Fig. 4, where the strong coupling constant are flavor-dependent. The root-mean-square deviations for the cases with unified strong coupling constant, flavor-dependent strong coupling constant and light baryons with $M<1.35$ GeV are indicated in the lower panel of Fig. 3, which are obtained with Eq. (33) at $N=18$, 18 and 12, respectively. As C increases, it is found that σ decreases if unified strong coupling constant is adopted. Meanwhile, as indicated in Fig. 4, the deviations from the experiment baryon masses increases with C for flavor-dependent strong coupling constant, *i.e.*, σ increases with C. Since we have fitted our parameters according to the masses of p, n, Λ, Δ, Σ and Ξ, the relative deviations are much smaller for light baryons with $M<1.35$ GeV in comparison to heavier ones. Then the root-mean-square deviation $\sigma\approx2.5$-3.9 MeV and is insensitive to the parameter sets adopted here. In such cases, we expect the model parameters indicated in Table 1 are best applied to systems with small baryon chemical potentials $\mu_b\lesssim1.35$ GeV.

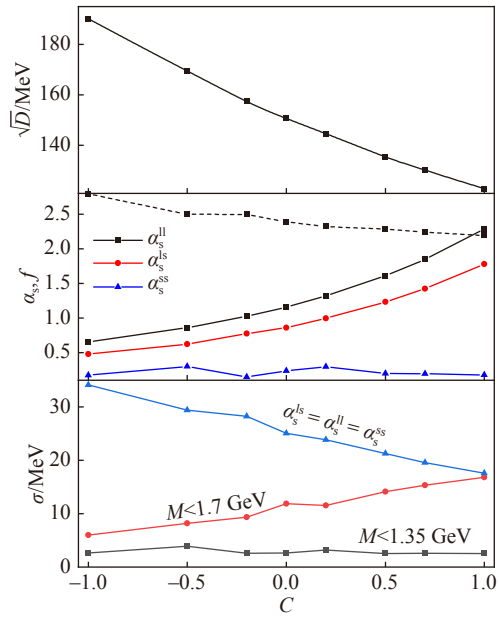

Fig. 3　The fitted parameters for the quark mass scaling in Eq. (10), the strong coupling constants, and mass the root-mean-square deviation σ as functions of parameter C. (color online)

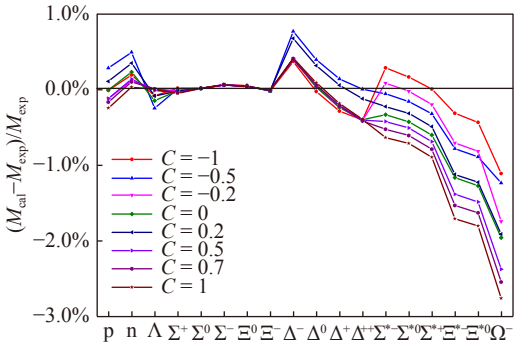

Fig. 4 The relative differences between the obtained masses of baryons and their experimental values. The baryons are all comprised of light quarks with masses $M_{exp} < 1.7$ GeV. (color online)

In Table 3 we present the mass gaps of baryons in various isospin-multiplets, which indicate the isospin breaking effects in baryons and are fixed by $M(I, I_3-1)-M(I, I_3)$ or $[M(I, I_3-2)-M(I, I_3)]/2$. The corresponding quark mass splitting is obtained with $\Delta m_{ud} = f(m_{d0}-m_{u0})$, where the mass factor f indicated in Table 1 is adopted. Evidently, the mass gaps in isospin-multiplets are generally small comparing with baryon masses, which is attributed to the small mass differences Δm_{ud} between u and d quarks. The mass gaps are dominated by Δm_{ud}, which are slightly dampened due to the nonzero kinetic energy of quarks. The Coulomb interaction contributes ~0.5-1 MeV to the masses of baryons with charge number $Q = \pm 1$, which reduces the mass splitting for nucleons N but increases for Ξ and Ξ*. The one-gluon-exchange interaction usually works against the isospin breaking effects except for Ξ, *e.g.*, the corresponding contributions to the mass splittings for N, Σ, Ξ, Δ, Σ* and Ξ* are −0.17, −0.02, 0.67, −0.17, −0.31 and −0.34 MeV at $C = 0$, respectively. Comparing with the experimental values, our model slightly overestimates the mass gaps for N, Σ, Σ*, Ξ* and underestimates that of Ξ. This could in principle be improved by reducing Δm_{ud}. In general, the mass gaps obtained in our equivparticle model vary little with respect to the adopted parameter sets and deviate slightly from the experimental values ($\lesssim 3$ MeV).

Table 3 Baryon and quark mass gaps (in MeV) of isospin-multiplets, which are fixed by varying the third component of isospin $\Delta I_3 = 1$.

C	−1	−0.5	−0.2	0	0.2	0.5	0.7	1	Exp.
N	3.4	3.4	3.8	3.8	4.1	4.1	4.2	4.2	1.3
Σ	4.4	4.4	4.6	4.6	4.8	4.7	4.9	4.8	4.0
Ξ	5.9	5.8	6.2	6.0	6.4	6.2	6.5	6.2	6.9
Δ	3.6	3.6	3.7	3.7	3.8	3.8	3.8	3.8	–
Σ*	4.4	4.4	4.3	4.3	4.2	4.2	4.1	4.2	2.2
Ξ*	5.2	5.3	4.9	5.0	4.7	4.9	4.6	4.8	3.2
Δm_{ud}	7.0	6.3	6.3	6.0	5.8	5.7	5.6	5.5	–

4 Conclusion

In this work we fix the parameter sets of equivparticle model including both confinement and leading-order perturbative interactions, which are attained by fitting to the mass spectra of baryons. Distinctive correlations of the confinement strength D, the strong coupling constant α_s, and the quark mass factor f with respect to the perturbative strength C are identified and can be well approximated by analytical formulae. Meanwhile, we have found that the color-magnetic part of one-gluon-exchange interaction is essential to explain the mass gap between baryons with spins $J = 1/2$ and 3/2, which reaches up to 300 MeV. Two sets of strong coupling constants for the one-gluon-exchange interaction between quarks are considered in this work, *i.e.*, unified and flavor-dependent ones. If larger perturbative strength C is adopted, the deviation of model calculations from experimental baryon masses increases for unified strong coupling constants and decreases for flavor-dependent ones. Based on the parameters fixed in this work, the equivparticle model gives good prediction on the masses of light baryons with $M < 1.35$ GeV, where the root-mean-square deviation is approximately 3 MeV and insensitive to the adopted parameter sets. We thus expect that the equivparticle model with constrained parameter sets are applicable to udQM nuggets, strangelets, and quark matter with small baryon chemical potentials $\mu_b \lesssim 1.35$ GeV.

Acknowledgments This work was supported by National SKA Program of China(Grant Nos. 2020SKA-0120300, 2020SKA0120100), National Natural Science Foundation of China(Grant Nos. 12275234, 12105241, 11875052, 12005005 & 12205093), and the Scientific Research Start-up Fund of Talent Introduction of Suqian University under Grant No. Xiao2022XRC061.

References:

[1] JAFFE R L. Phys Rev Lett, 1977, 38: 195.
[2] JAFFE R L. Phys Rev Lett, 1977, 38: 617.
[3] AERTS A T M, MULDERS P J G, DE SWART J J. Phys Rev D, 1978, 17: 260.
[4] MULDERS P J, AERTS A T, DE SWART J J. Phys Rev D, 1980, 21: 2653.
[5] LIU K, WONG C. Phys Lett B, 1982, 113(1): 1.
[6] MALTMAN K. Phys Lett B, 1992, 291(4): 371.
[7] MAEZAWA Y, HATSUDA T, SASAKI S. Prog Theor Phys, 2005, 114: 317.
[8] OKA M, SHIMIZU K, YAZAKI K. Phys Lett B, 1983, 130: 365.
[9] STRAUB U, ZHANG Z Y, BRAUER K, et al. Phys Lett B, 1988, 200: 241.
[10] OKA M, TAKEUCHI S. Nucl Phys A, 1991, 524: 649.
[11] SHEN P, ZHANG Z, YU Y, et al. J Phys G, 1999, 25: 1807.
[12] BALACHANDRAN A P, BARDUCCI A, LIZZI F, et al. Phys Rev

Lett, 1984, 52: 887.
[13] JAFFE R, KORPA C. Nucl Phys B, 1985, 258: 468.
[14] YOST S A, NAPPI C R. Phys Rev D, 1985, 32: 816.
[15] KOPELIOVICH V, SCHWESINGER B, STERN B. Nucl Phys A, 1992, 549: 485.
[16] LEE S H, YASUI S. Eur Phys J C, 2009, 64: 283.
[17] SAKAI T, MORI J, BUCHMANN A, et al. Nucl Phys A, 1997, 625(1): 192.
[18] GLENDENNING N K, SCHAFFNER-BIELICH J. Phys Rev C, 1998, 58: 1298.
[19] LAI X Y, XU R X. Mon Not Roy Astron Soc, 2009, 398(1): L31.
[20] ZHANG Q R, LIU H M. Phys Rev C, 1992, 46: 2294.
[21] MIAO Z Q, XIA C J, LAI X Y, et al. Int J Mod Phys E, 2022, 31(4): 2250037.
[22] CHODOS A, JAFFE R L, JOHNSON K, et al. Phys Rev D, 1974, 10: 2599.
[23] FARHI E, JAFFE R L. Phys Rev D, 1984, 30: 2379.
[24] NAMBU Y, JONA-LASINIO G. Phys Rev, 1961, 122: 345.
[25] FRAGA E S, KURKELA A, VUORINEN A. Astrophys J, 2014, 781(2): L25.
[26] PLUMARI S, BURGIO G F, GRECO V, et al. Phys Rev D, 2013, 88: 083005.
[27] GOLOVIZNIN V, SATZ H. Z Phys C, 1993, 57(4): 671.
[28] GORENSTEIN M I, YANG S N. Phys Rev D, 1995, 52: 5206.
[29] SCHERTLER K, GREINER C, THOMA M. Nucl Phys A, 1997, 616(3–4): 659.
[30] PESHIER A, KÄMPFER B, SOFF G. Phys Rev C, 2000, 61: 045203.
[31] BANNUR V M. Phys Rev C, 2007, 75: 044905.
[32] GARDIM F, STEFFENS F. Nucl Phys A, 2009, 825: 222.
[33] FOWLER G N, RAHA S, WEINER R M. Z Phys C, 1981, 9: 271.
[34] PLüMER M, RAHA S, WEINER R. Phys Lett B, 1984, 139(3): 198.
[35] CHAKRABARTY S, RAHA S, SINHA B. Phys Lett B, 1989, 229(1–2): 112.
[36] BENVENUTO O G, LUGONES G. Phys Rev D, 1995, 51: 1989.
[37] PENG G X, CHIANG H C, ZOU B S, et al. Phys Rev C, 2000, 62: 025801.
[38] SASAKI K, AOKI S, DOI T, et al. Nucl Phys A, 2020, 998: 121737.
[39] GREEN J R, HANLON A D, JUNNARKAR P M, et al. Phys Rev Lett, 2021, 127: 242003.
[40] BODMER A R. Phys Rev D, 1971, 4: 1601.
[41] WITTEN E. Phys Rev D, 1984, 30: 272.
[42] TERAZAWA H. J Phys Soc Jpn, 1989, 58(10): 3555.
[43] DEXHEIMER V, TORRES J, MENEZES D. Eur Phys J C, 2013, 73(9): 2569.
[44] BERGER M S, JAFFE R L. Phys Rev C, 1987, 35: 213.
[45] GILSON E P, JAFFE R L. Phys Rev Lett, 1993, 71: 332.
[46] PENG G X, WEN X J, CHEN Y D. Phys Lett B, 2006, 633(2–3): 314.
[47] RúJULA A D, GLASHOW S L. Nature (London), 1984, 312: 734.
[48] LOWDER D M. Nucl Phys B (Proc Suppl), 1991, 24(2): 177.
[49] RAFELSKI J, LABUN L, BIRRELL J. Phys Rev Lett, 2013, 110: 111102.
[50] ITOH N. Prog Theor Phys, 1970, 44(1): 291.
[51] ALCOCK C, FARHI E, OLINTO A. Astrophys J, 1986, 310: 261.
[52] HAENSEL P, ZDUNIK J L, SCHAEFFER. R. Astron Astrophys, 1986, 160: 121.
[53] BUBALLA M, OERTEL M. Phys Lett B, 1999, 457(4): 261.
[54] KLÄHN T, FISCHER T. Astrophys J, 2015, 810(2): 134.
[55] HOLDOM B, REN J, ZHANG C. Phys Rev Lett, 2018, 120: 222001.
[56] XIA C J, XUE S S, XU R X, et al. Phys Rev D, 2020, 101(10): 103031.
[57] WANG L, HU J, XIA C J, et al. Galaxies, 2021, 9(4): 70.
[58] ZHAO T, ZHENG W, WANG F, et al. Phys Rev D, 2019, 100: 043018.
[59] ZHANG C. Phys Rev D, 2020, 101: 043003.
[60] CAO Z, CHEN L W, CHU P C, et al. arXiv: 2009.00942, 2020.
[61] ZHANG C, MANN R B. Phys Rev D, 2021, 103: 063018.
[62] YUAN W L, LI A, MIAO Z, et al. Phys Rev D, 2022, 105: 123004.
[63] CAO Z, CHEN L W, CHU P C, et al. Phys Rev D, 2022, 106: 083007.
[64] PENG G X, CHIANG H C, YANG J J, et al. Phys Rev C, 1999, 61: 015201.
[65] WANG P. Phys Rev C, 2000, 62: 015204.
[66] ZHANG Y, SU R K, YING S Q, et al. Europhys Lett, 2001, 56(3): 361.
[67] LUGONES G, HORVATH J E. Int J Mod Phys D, 2003, 12: 495.
[68] WEN X J, ZHONG X H, PENG G X, et al. Phys Rev C, 2005, 72: 015204.
[69] WEN X J, PENG G X, CHEN Y D. J Phys G, 2007, 34(7): 1697.
[70] YIN S, SU R K. Phys Rev C, 2008, 77: 055204.
[71] CHEN S W, GAO L, PENG G X. Chin Phys C, 2012, 36(10): 947.
[72] TORRES J R, MENEZES D P. Europhys Lett, 2013, 101(4): 42003.
[73] CHANG Q, CHEN S W, PENG G X, et al. Sci China-Phys Mech Astron, 2013, 56(9): 1730.
[74] XIA C J, CHEN S W, PENG G X. Sci China-Phys Mech Astron, 2014, 57(7): 1304.
[75] XIA C J, PENG G X, CHEN S W, et al. Phys Rev D, 2014, 89: 105027.
[76] CHU P C, CHEN L W. Astrophys J, 2014, 780(2): 135.
[77] HOU J X, PENG G X, XIA C J, et al. Chin Phys C, 2015, 39: 015101.
[78] PENG C, PENG G X, XIA C J, et al. Nucl Sci Tech, 2016, 27(4): 98.
[79] CHU P C, CHEN L W. Phys Rev D, 2017, 96: 083019.
[80] Particle Data Group. Chin Phys C, 2016, 40(10): 100001.
[81] Particle Data Group. Prog Theor Exp Phys, 2020, 2020: 083C01.
[82] COHEN T D, FURNSTAHL R J, GRIEGEL D K. Phys Rev C, 1992, 45: 1881.
[83] JEONG K S, LEE S H. Nucl Phys A, 2016, 945: 21.
[84] CHEN L W. Nucl Phys Rev, 2017, 34: 20.
[85] CHU P C, ZHOU Y, QI X, et al. Phys Rev C, 2019, 99: 035802.
[86] WU X, OHNISHI A, SHEN H. AIP Conf Proc, 2019, 2127(1): 020032.
[87] BARTELSKI J, SZYMACHA A, MANKIEWICZ L, et al. Phys Rev D, 1984, 29: 1035.
[88] BENDER M, RUTZ K, REINHARD P G, et al. Eur Phys J A, 2000, 7(4): 467.
[89] ALFORD M G, SCHMITT A, RAJAGOPAL K, et al. Rev Mod

Phys, 2008, 80: 1455.
[90] WANG F, WU G H, TENG L J, et al. Phys Rev Lett, 1992, 69: 2901.
[91] BERNOTAS A, ŠIMONIS V. Nucl Phys A, 2004, 741: 179.

等效质量模型中的重子质量谱

尤浩松[1], 夏铖君[1,†], 朱新梅[1], 陈鹏辉[1], 徐建峰[2], 陆振烟[3], 彭光雄[4,5,6], 徐仁新[7,8]

(1. 扬州大学物理科学与技术学院，江苏 扬州 225009；
2. 宿迁学院信息工程学院，江苏 宿迁 223800；
3. 湖南科技大学物理与电子科学学院，湖南 湘潭 411201；
4. 中国科学院大学核科学技术学院，北京 100049；
5. 中国科学院高能物理研究所大科学装置理论物理研究中心，北京 100049；
6. 湖南师范大学量子效应及其应用协同创新中心，长沙 410081；
7. 北京大学物理学院，北京 100871；
8. 北京大学卡夫利天文学和天体物理学研究所，北京 100871)

摘要: 在等效质量模型框架下，考虑线性禁闭和一阶微扰相互作用的贡献并通过拟合 p、n、Λ 和 Δ 的质量来得到模型参数。发现，等效质量模型能够较好地给出符合实验的重子质量谱。而禁闭强度 D、强耦合常数 α_s 以及夸克质量因子 f 与微扰强度 C 之间都存在关联，并能够很好地用解析公式逼近。除此之外，单胶子交换相互作用的色磁部分在重子质量谱中起着重要作用，从而使自旋 $J = 1/2$ 和 3/2 的重子之间的质量差最高达到 300 MeV。为了更好地描述超子质量，对于包含奇异夸克的一对夸克间的相互作用我们进一步采用不同的强耦合常数，其具体的模型参数通过拟合 Σ 和 Ξ 的质量得到。基于本工作得到的等效质量模型参数组，能够更好地描述 ud 夸克物质团、奇异子以及致密星。

关键词: 重子质量谱；等效质量模型；单胶子交换相互作用

收稿日期: 2022-08-02； **修改日期:** 2022-08-20

基金项目: 国家重点研发计划 SKA 专项项目 (2020SKA0120300, 2020SKA0120100)；国家自然科学基金资助项目 (12275234, 12105241, 11875052, 12005005, 12205093, 11673002)；宿迁学院人才引进科研启动基金 (Xiao2022XRC061)

† **通信作者:** 夏铖君，E-mail: cjxia@yzu.edu.cn